

<https://doi.org/10.1038/s42003-025-07477-2>

Thermal variation influences the transcriptome of the major malaria vector *Anopheles stephensi*

Check for updates

Ashutosh K. Pathak^{1,2,3,7}✉, Shannon Quek^{4,7}, Ritu Sharma², Justine C. Shiao^{1,2,3}, Matthew B. Thomas⁵, Grant L. Hughes⁴ & Courtney C. Murdock^{1,2,3,6}

The distribution and abundance of ectothermic mosquitoes are strongly affected by temperature, but mechanisms remain unexplored. We describe the effect of temperature on the transcriptome of *Anopheles stephensi*, an invasive vector of human malaria. Adult females were maintained across a range of mean temperatures (20 °C, 24 °C and 28 °C), with daily fluctuations of +5 °C and –4 °C at each mean temperature. Transcriptomes were described up to 19 days post-blood meal. Of the >3100 differentially expressed genes, we observed shared temporal expression profiles across all temperatures, suggesting their indispensability to mosquito life history. Tolerance to 20 and 28 (+ 5 °C/–4 °C) was associated with larger and more diverse transcriptomes compared to 24 (+ 5 °C/–4 °C). Finally, we identified two distinct trends in gene expression in response to blood meal ingestion, oxidative stress, and reproduction. Our work has implications for mosquitoes' response to thermal variation, mosquito immune-physiology, mosquito-malaria interactions and the development of vector control tools.

Climate change is expected to lead to the redistribution of mosquito species on a global scale. While climate change is the cumulative effect of several environmental factors, changes in temperature have been demonstrated in numerous studies to be one of the most important factors constraining the distribution and abundance of ectothermic organisms^{1–7}. For mosquitoes, and ectotherms more generally, the relationship between temperature and the performance of traits relevant for lifetime fitness is unimodal, where performance increases until the optimum temperature is reached, after which it starts to decline (reviewed in ref. 8). Based on the metabolic theory of ecology, as temperatures warm toward the thermal optimum, the rate and efficiency of enzymatic processes will increase. Beyond the thermal optimum, enzymatic processes are predicted to become less efficient due to protein misfolding or desiccation stress until the critical upper temperature is reached, where organismal death occurs⁷. However, the physiological mechanisms underlying this unimodal response remain unclear. Identifying these mechanisms is pertinent for at least three reasons. First, to understand the mechanisms underpinning the plasticity of mosquitoes to respond to different temperatures. Second, to provide more reference points for local adaptation within and between

species. Third, to determine if the gene(s) that ultimately mediate these physiological responses could be selectively inherited in response to the current trends in climate change⁹.

Despite the implications for public health, few studies have identified the genetic basis for how mosquitoes respond to temperature^{10,11}. Several species within the genus *Anopheles* are important vectors of human malaria, which continues to cause significant morbidity and mortality¹². Environmental temperature regulates the rates of parasite establishment and development, as well as mosquito traits that govern mosquito population and transmission dynamics^{13–18}. The thermal performance curves of mosquitoes are also unimodal with mosquito species differing significantly in thermal breadth^{13,14,18–20}. Amongst *Anopheles*, *An. stephensi* is considered a major vector for *Plasmodium* parasites²¹ in South Asia and, more recently, in urban centers of Africa^{21,22}. In addition to this species' relatively unique ability to develop in water storage containers, its thermal breadth is also thought to have contributed to its success in establishing warmer and drier environments than other *Anopheles*²¹. Whether this thermotolerance is associated with *An. stephensi* can be explained by transcriptional responses has not been assessed.

¹Department of Infectious Diseases, University of Georgia, Athens, GA, USA. ²Center for Tropical and Emerging Global Diseases, University of Georgia, Athens, GA, USA. ³Center for Ecology of Infectious Diseases, University of Georgia, Athens, GA, USA. ⁴Departments of Vector Biology and Tropical Disease Biology, Centre for Neglected Tropical Disease, Liverpool School of Tropical Medicine, Liverpool, UK. ⁵Department of Entomology & Nematology, Invasion Science Research Institute, University of Florida, Gainesville, FL, USA. ⁶Present address: Department of Entomology, Cornell University, Ithaca, NY, USA. ⁷These authors contributed equally: Ashutosh K. Pathak, Shannon Quek. ✉e-mail: ash1@uga.edu

Physiological mechanisms underlying fitness traits are often the product of multiple genes and interacting pathways^{23,24}. However, most of our understanding of the thermal responses of mosquitoes is derived from species housed at constant temperatures. A few studies have shown the total number of genes and overall profiles can vary significantly between ectotherms housed at constant temperatures compared to fluctuating conditions^{25–27}. Resolving responses in realistic environments is essential to the understanding of how ectotherms, like mosquitoes, respond to field-relevant variation in temperature²⁸.

In the current study, we use a bulk RNAseq approach to describe how variation in temperature modulates global gene expression profiles in *An. stephensi* maintained under field-relevant diurnally fluctuating temperature regimes (DTR herein) around mean temperatures of 20 °C, 24 °C and 28 °C, with 24 °C being closest to the predicted thermal optimum (T_{opt}) for malaria transmission potential (~ 25°C)^{13,15}. We asked the following three questions in this experimental study. First, how do transcriptional responses change

over time in response to field-relevant variations in ambient temperature? Second, do mosquito transcriptional responses exhibit distinct temporal dynamics in response to temperature variation. Third, can temperature influence gene expression profiles at spatially and functionally distinct local (midgut) and systemic/organismal levels (carcasses)? The results that we find in this study have important implications for how temperature variation affects key life history processes, as well as how we characterize mosquito immune-physiology and mosquito-malaria interactions, and for the development of novel vector control tools.

Methods

Study design

For a schematic of the study design, refer to Fig. 1A. Two days before the blood meal, 500, 3–5-day old female, host-seeking *An. stephensi* were aspirated into each of three polyester cages (32.5 cm³, BugDorm, Taiwan). Each of the 3 cages was transferred to environmental chambers (Percival

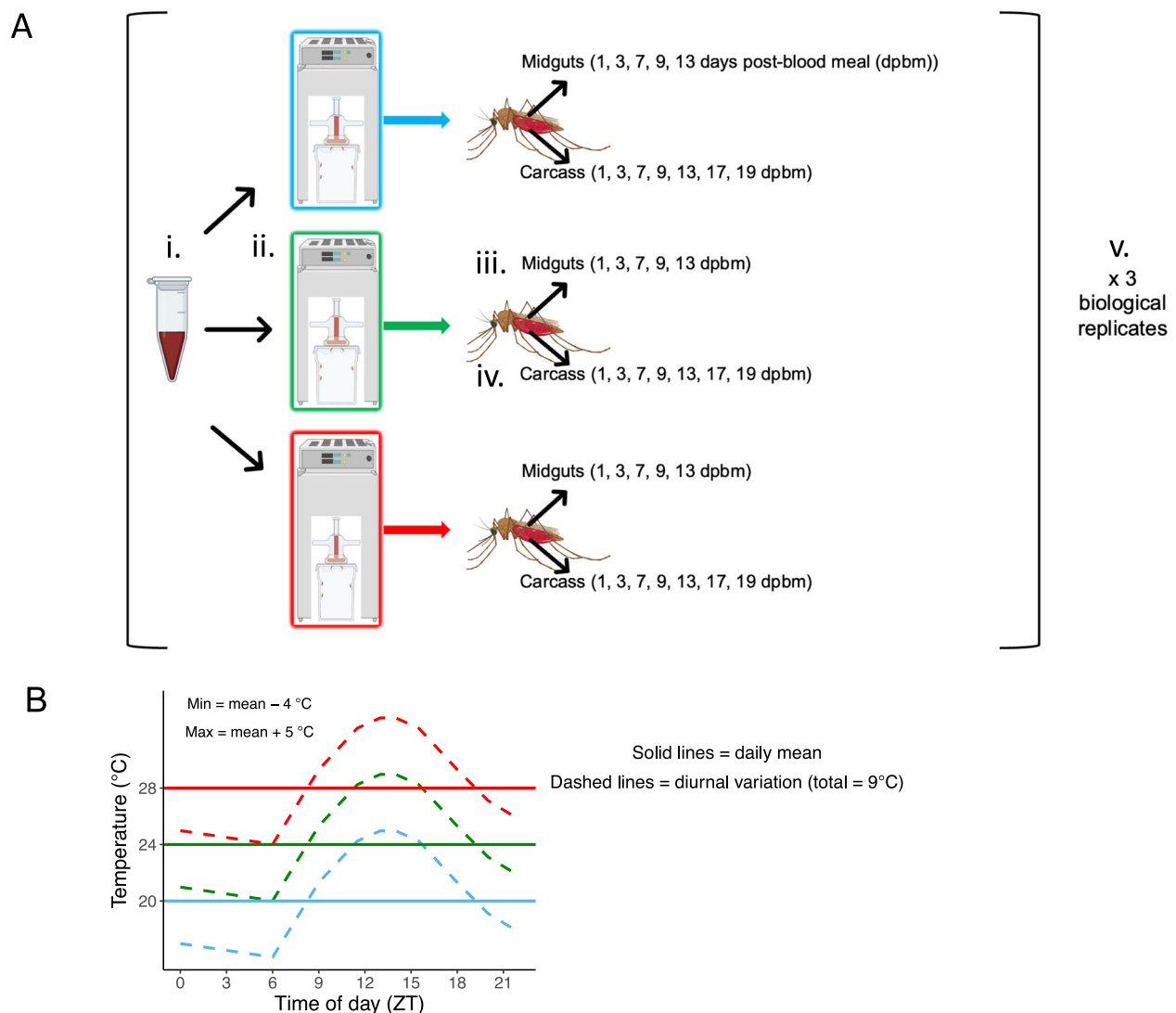


Fig. 1 | Overview of study design and temperature regimes. General experimental design (A) and temperature regimes (B). A 500 female, *An. stephensi* were (i) offered blood meals at ZT18 hours (B) and (ii), returned to environmental chambers maintained at the three temperature regimes (= day 0 post-blood meal), as described previously^{15,29}. At days 1, 3, 7, 9, 13, 17 and 19 post-blood meal, (iii) midguts were first pooled from 10 individuals at each temperature (“Midguts”), following which (iv), all the remaining tissues (i.e., whole mosquito except the midgut) from these 10 individuals were pooled into another collection tube (“Carcass”); in other words, at each time-point, we collected 6 samples for RNAseq,

with 1 sample each of midguts and carcasses (total = 2) at each of the three temperatures ($2 \times 3 = 6$); however, note that only carcasses were collected on days 17 and 19 post-blood meal. Finally, (v) samples were collected from 3 cohorts of mosquitoes. Therefore, in each replicate, RNAseq was performed with 36 samples: 15 midgut pools representing 1, 3, 7, 9, and 13 post-blood meal (5 pools at each temperature), and 21 carcass pools representing days 1, 3, 7, 9, 13, 17, and 19 post-blood meal (7 pools at each temperature). Together, the three replicates resulted in a total of 108 samples for RNAseq. Schematic in (A) was created with BioRender.com.

Scientific, Perry, IA) maintained at the 3 temperature regimens (Fig. 1B). After mosquitoes had been acclimated to the three temperatures for 48 h, blood meals were performed at ZT18 hours (Fig. 1A) with washed human RBCs reconstituted with human serum (Valley Biomedical, Winchester, VA), as described previously^{15,29}. Mosquitoes were allowed to feed for 15 min, and fully engorged mosquitoes then returned to the respective temperature regime (Fig. 1B).

At ZT15 hours (Fig. 1B) on days 1, 3, 7, 9, 13, 17 and 19 post-blood meal (Fig. 1B), a sub-sample of ~20–25 mosquitoes were collected from the cage at each of the three temperatures. At each time-point, the midguts of 10 gravid individuals were dissected and pooled from each temperature (“midguts”) so that transcriptional profiles could be generated for the tissue interacting most closely with blood meal digestion. To generate systemic transcriptional profiles, the remaining mosquito tissues from these 10 individuals were pooled into a separate collection tube (carcasses herein) (Fig. 1B), also for RNAseq; note that only carcasses were collected on days 17 and 19 post-blood meal.

The sampling schedule above was repeated across three biological replicates. Therefore, in each replicate, RNAseq was performed with 36 samples: 15 midgut pools representing 1, 3, 7, 9 and 13 post-blood meal (5 pools at each temperature), and 21 carcass pools representing days 1, 3, 7, 9, 13, 17 and 19 post-blood meal (7 pools at each temperature). Together, the three replicates resulted in a total of 108 samples for RNAseq.

Mosquito husbandry, blood feeds, and sample collections

Unless stated otherwise, all chemicals and consumables were purchased from Thermo-Fisher Scientific (Waltham, MA). As described previously^{15,29}, our colony of *An. stephensi* was initiated from eggs kindly provided by the Walter Reed Army Institute of Research ca. 2015. This is a wild-type strain referred to as strain “Indian”³⁰. Routine mosquito husbandry was performed as described previously^{15,29}. Briefly, colonies were propagated on a weekly basis with eggs oviposited by mosquitoes offered packed, O+ human RBCs supplemented with freshly thawed A+ human serum (Valley Biomedical, Winchester, VA), just prior to the blood meal. Larvae were propagated on a progressive feeding schedule of Hikari Cichlid Gold medium pellets (Hikari Inc, Hayward, CA), while adults were routinely maintained on 5% dextrose (w/v) and 0.05% PABA (w/v). As mentioned above, ~20–25 mosquitoes from each cage were directly aspirated into 70% ethanol, with midguts and carcasses pooled into 50 μ L and 500 μ L of RNeasy lysis buffer respectively. After overnight storage at 2–4 °C, samples were transferred to –80 °C until RNA purification and sequencing.

RNA purification and sequencing

Total RNA was purified from the midguts and carcasses with commercially available kits (PureLink RNA Mini Kit) as recommended by the manufacturer (Thermo-Fisher Scientific, Waltham, MA). RNA sequencing (RNAseq herein) was performed by the Georgia Genomics and Bioinformatics Core (GGBC) at the University of Georgia (Athens, GA). The concentration and integrity of total RNA were assessed with a Bioanalyzer (Thermo-Fisher Scientific, Waltham, MA). Libraries for RNAseq were prepared for each sample with a KAPA stranded mRNA-seq kit as per manufacturer’s recommendations (Roche, Indianapolis, IN); briefly, mRNA was first selected with oligo-dT beads, followed by fragmentation of the RNA prior to generating cDNA using random hexamer priming. The quality and quantity of each library were estimated with a qubit or plate reader before pooling for RNAseq. Pooled libraries were run on a NextSeq 550 (Illumina Inc., San Diego, CA). De-multiplexing and trimming of adapter and barcode sequences were performed on BaseSpace (Illumina Inc., San Diego, CA).

Statistics and reproducibility

Sequence data were obtained in fastq format, and read quality was confirmed using FASTQC v0.11.5³¹, with all samples showing an average PHRED score >30 and no adapter sequences detected. Samples that showed <1 million sequenced reads were not included in subsequent differential

expression analysis due to concerns about accurate quantification of gene expression. Sequences were aligned to the *Anopheles stephensi* “Indian” strain reference genome (genome version GCA_000300775.2, annotation version AsteI2.3) using the program Hisat2 (v2.1.0)³². FeatureCounts v2.0.1³³ was used to obtain raw read count-data from the sequencing files. The resulting feature count table was then processed using the program DESeq2 (v1.30.1)³⁴ in R (v4.3.0)³⁵. DESeq2 automatically performs filtering of genes with low read counts to increase statistical power, as well as normalization of gene expression based on the raw count-data. This was used to generate a PCA plot and sample-to-sample distance matrices in DESeq2 for further quality control and identification of sample clustering. Five samples appeared as distinct outliers in both analyses (no clustering with any biological replicate or any other sample) and were thus excluded from subsequent differential expression analysis. Despite sample removals based on low read counts or outliers from the remaining samples, all experimental conditions had a minimum of two biological replicates for differential expression analysis.

To investigate the impact of temperature on gene expression in mosquitoes over the course of the experiment (19 days), we utilized DESeq2’s in-built likelihood ratio test (LRT)³⁴. This type of test can be useful in analyzing time-course experiments, as it evaluates expression change across multiple experimental factors. The LRT test looks at gene expression profiles and identifies genes that show differences in both expression as well as patterns across temperatures. i.e., genes that show changes in expression level but have the same broad pattern over time, would be considered as non-significant.

To first investigate gene changes over time at the three different temperatures, we treated each mosquito cohort at the different temperatures as a separate time-series experiment, with a design formula of ~Time, reduced formula of ~1, and adjusted *p*-value cutoff of 0.05. No thresholds of log₂ fold-changes were applied, as we were also interested in investigating the influence of small changes across an entire pathway. This analysis was performed for both guts and carcasses separately. The resultant list of differentially expressed genes was then used to create an Upset plot using the UpsetR package v1.4.0³⁶ to visualize the number of differentially expressed genes at the different temperatures and overlaps among them. These overlaps indicated the presence of clusters of genes that may show differential expression based on temperature.

To identify genes that may be clustering together based on gene expression, as well as visualize these changes over time, we utilized a technique known as *K*-means clustering via the MFuzz package (v2.60.0)³⁷. This is a technique used for soft-clustering analysis of data and allows subsequent illustration of gene expression profiles (GEPs) in time-series data. MFuzz requires as input normalized count-data, taken from DESeq2³⁴, as well as a user-defined number of “cluster cores”, which defines the number of GEPs to be drawn. Too few cluster cores will result in reduced sensitivity for finding unique GEPs, while too many cluster cores will result in redundant patterns. Normalized count-data for the statistically significantly differentially expressed genes for each of the different temperatures and tissues were used—other genes that did not meet an adjusted *p*-value of 0.05 were discarded for this analysis. For the identification of cluster cores, we performed clustering analysis using an increasing number of cluster cores and scored the correlation of the resulting clusters using the “cor” function of base R stats package³⁵. The number of cluster cores to use was determined by a maximum correlation score of 0.85, where a correlation score of 1 indicates perfect match of the gene expression profile, and a score of –1 indicates a perfect inversion of the profile. This resulted in between 3 to 5 cluster cores depending on the analysis being investigated, with their corresponding expression profiles drawn using MFuzz³⁷ and the ggplot2 package³⁸. For identifying changes in expression, identified GEPs were compared against one another, both in terms of profile and the gene lists associated with them to see how genes may change expression profiles depending on temperature. Gene lists from each GEP were then processed for gene ontology enrichment to assign functions for each profile using the g:Profiler web server³⁹, with a significance cutoff of 0.05.

Reporting summary

Further information on research design is available in the Nature Portfolio Reporting Summary linked to this article.

Results

At 28 DTR 9 °C, mosquito survival begins to decline rapidly ~15–17 days post-blood meal^{15,18,28,40–42}, and thus, to ensure availability of sufficient material for RNAseq (and from same number of mosquitoes across all three temperatures), sampling was performed until 19 days post-blood meal. The time-points spanning this 19-day time period were chosen to capture temperature-dependent gene expression profiles associated with blood meal digestion and oogenesis (days 1, 3 and potentially 7 days post-blood meal for 20 DTR 9 °C)^{14,28}, as well as chronological/physiological aging (day 7 onwards). From all experimental conditions (Fig. 1), we acquired between 4302 to 128,645,661 reads, with five samples showing less than one million sequenced reads. Furthermore, initial PCA clustering of counts results showed six samples that appeared as clear outliers in the data and did not cluster with any other data point. These eleven samples were removed from downstream differential expression analysis.

Variation in transcriptomes exhibit differences across time and tissues

The effect of temperature on overall gene expression profiles at each time-point in carcasses and midguts was investigated. The PCA plot indicated two major clustering factors that together accounted for 61% of the overall variation in the data (Fig. 2A). The first principal component (PC1) was the site of sampling (36% variance), with gene expression profiles at the site of blood meal ingestion (midguts) distinct from the systemic responses (carcasses) (Fig. 2, ovals with solid line); in general, profiles were more variable between the midguts. The second principal component was time (25% variance), with distinct gene expression profiles at day 1 after receiving the blood meal compared to the later time-points (Fig. 2A, ovals with dotted line).

Tolerance to cooler (20 DTR 9 °C) and warmer (28 DTR 9 °C) temperatures was associated with a larger repertoire of gene products than the more optimal 24 DTR 9 °C

Likelihood Ratio Tests were used to analyze the data as a time-series to capture genes that showed statistically significant deviation in expression patterns at the three different temperatures. This also allowed for subsequent clustering of these patterns and comparisons between the different temperatures analyzed. From this analysis, 1798, 1341 and 1671 genes were identified as statistically significantly differentially expressed in the carcasses at 20, 24 and 28 DTR 9 °C, respectively. In the midguts, 2810, 1418 and 1995 genes were differentially expressed at 20, 24 and 28 DTR 9 °C. These genes were not necessarily unique per temperature, and organ assayed, with up to 902 genes shared across the analyzed temperatures in various combinations (Fig. 2B, C).

Next, likelihood ratio tests were used to identify genes that showed statistically significant changes in expression patterns over time at the three different temperature treatments. In the carcasses, a total of 3106 unique genes were identified across the different temperatures, when aggregated over time. Of the genes unique to each temperature, a significantly higher number of differentially expressed genes were recovered at the low and high temperatures of 20 DTR 9 °C and 28 DTR 9 °C (849 and 720, respectively), compared to 24 DTR 9 °C (282) (Fig. 2B). While 449 genes were shared across all three temperatures, the remaining genes showed similar patterns between at least two of the three temperatures (e.g., the 306 between 24 DTR 9 °C and 28 DTR 9 °C, or the 304 genes across 20 DTR 9 °C and 24 DTR 9 °C) (Fig. 2B).

Analyses of the midguts identified a total of 3590 unique genes with clear differences in expression levels over the three temperatures aggregated over time. Unlike the carcasses, the largest group of significant genes were found at 20 °C DTR 9 °C (1223 genes), with the second-largest group represented by genes that were shared across all temperatures (902 genes)

(Fig. 2C). While 464 genes were still unique to 28 DTR 9 °C, like the carcasses, only 172 genes were expressed exclusively in the midguts of mosquitoes housed at 24 DTR 9 °C. The remaining 829 genes from the 3590 total were shared between at least two of the three temperatures (Fig. 2C).

Temporal classification of differentially expressed genes reveals clusters of shared and unique genes in the carcasses and midguts of mosquitoes at all three temperatures

To get a higher resolution of how temperature affects variation in the temporal dynamics of gene expression, specific group(s) of unique and shared genes identified above (Fig. 2) were analyzed using *K*-means clustering. This separated each group of genes into 3–5 “clusters” based on the similarity in expression profiles over time. We first looked at the temporal clustering profiles of the genes uniquely expressed in carcasses at each temperature. The 849 (20 DTR 9 °C), 282 (24 DTR 9 °C), and 720 (28 DTR 9 °C) genes uniquely expressed in the carcasses at each temperature (Fig. 2B) could be separated into 3–4 clusters per temperature (Fig. 3A–C), with between 64 to 347 genes in each cluster (Table 1). Similar clusters were also derived from the differentially expressed genes in the midguts of mosquitoes at days 1, 3, 7, 9 and 13 after the blood meal. For the 1223 (20 DTR 9 °C), 172 (24 DTR 9 °C) and 464 (28 DTR 9 °C) genes uniquely expressed in the midguts at each temperature (Fig. 2C), 3–5 gene clusters were identified per temperature (Fig. 3D–F) with sizes ranging from 42–313 genes per cluster (Table 1). For both carcasses and midgut gene expression analyses, the threshold criteria used to generate clusters accounted for 100% of the unique genes at each temperature.

Amongst the differentially expressed genes in the carcasses, the expression of 449 genes were shared across all three temperatures (Fig. 2B). Grouping these genes based on temporal expression profiles revealed three clusters at each temperature, with majority of the genes falling into cluster 3 (317, 20 DTR 9 °C; 381, 24 DTR 9 °C; and 295 genes, 28 DTR 9 °C; Fig. 4A) (Table 2). In the midguts, we observed a higher number of shared genes (902 genes), with 4 clusters at each temperature ranging in size from 111–475 genes with similarities in temporal expression profiles (Fig. 4B and Table 2).

Transcriptomic responses to the blood meal reveal two complementary trends across all gene clusters at both sampling sites and all temperature regimens

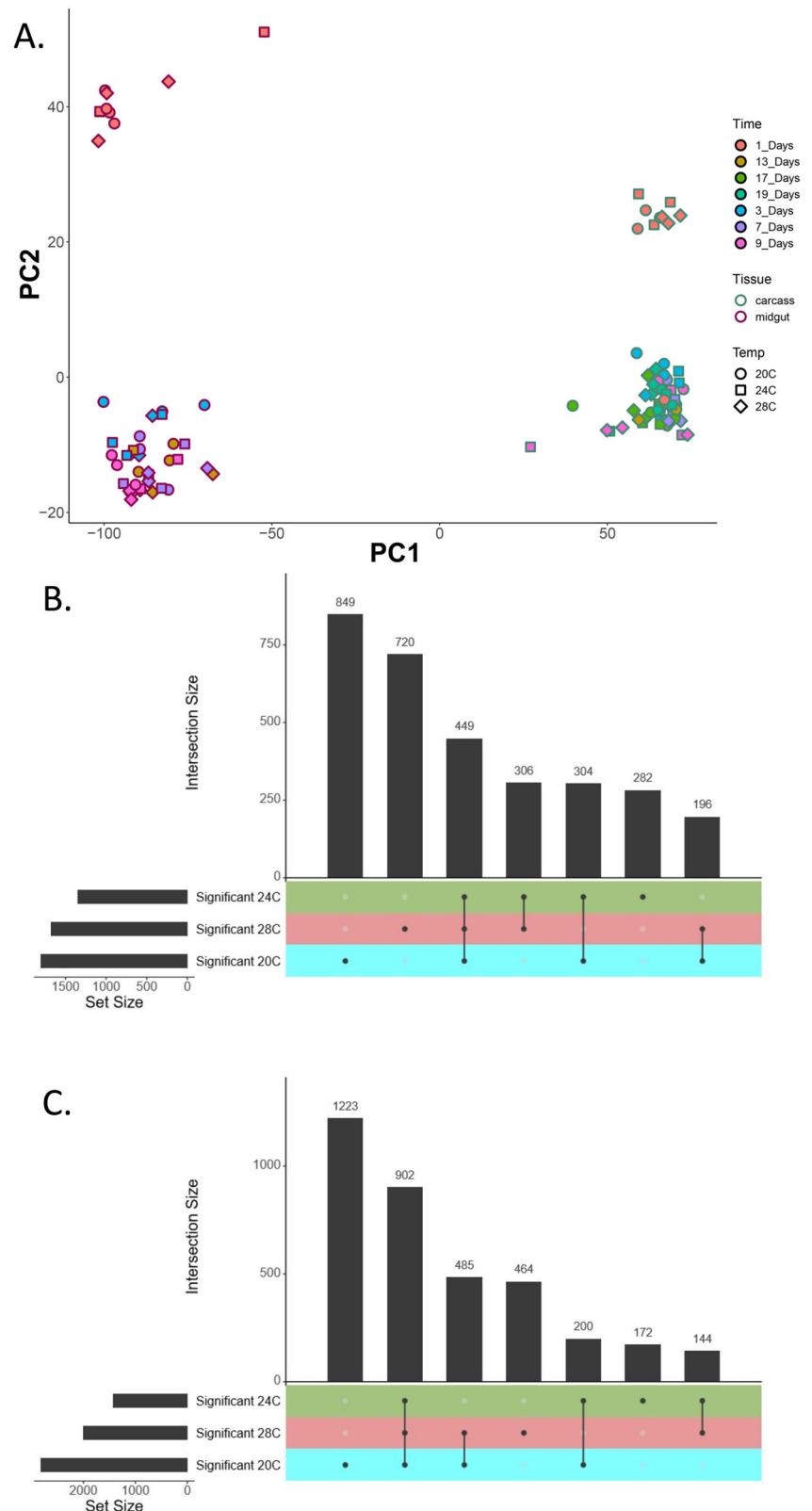
A visual comparison of the expression profiles suggested two general trends in expression across the unique and shared gene clusters in the carcasses and midguts at all three temperatures (Fig. 3, top-right key and listed in Table 1 in a column titled “Inferred trend”). The first trend (Trend 1) was characterized by gene clusters that were enriched a day after the blood meal before returning to expression levels below the averages for the rest of the sampling period. The second trend (Trend 2), by contrast, represents gene clusters that were depleted 1 day after the blood meal but subsequently showed variable expression patterns over the remaining time-points, often increasing in expression.

Functional profiling of the gene clusters was performed with Gene ontology (GO) enrichment analysis. GO profiling was not possible for all the clusters, especially for some of the uniquely expressed clusters (Table 1) (refer to Supplementary Data 1 for detailed output of GO analyses, and Supplementary Data 2 for list of protein-coding genes corresponding to the GO terms in each cluster). However, of the 2941 genes suggested by the GO analysis (Supplementary Data 2), we restrict our discussion to the 732 genes that were annotated by VectorBase.org, i.e., genes expressing products with known functions.

Functional profiling of Trend 1 genes in carcasses

Functional profiling of genes in clusters expressed in (i), carcasses, (ii), unique to each temperature and (iii), following Trend 1. Amongst the unique gene clusters that were members of Trend 1 (enriched a day after the blood meal, followed by depletion at all other time-points) includes cluster 2 at 20 DTR 9 °C (237 genes) (Fig. 3A). Analysis of GO enrichment for this profile suggested coordinated regulation of the

Fig. 2 | Summary plots showing characteristics of differentially expressed genes in carcasses and midguts of *An. stephensi* across different temperatures and times. **A** PCA plot illustrating similarities and differences between samples. Note the distinction between carcasses and midguts (“Tissue”), as well as Day 1 versus other time-points (“Time”). **B** UpsetR plot showing how genes in carcasses show unique or shared statistically significant differential expression at certain temperatures between 20 DTR 9 °C, 24 DTR 9 °C and 28 DTR 9 °C. UpsetR plots are an alternative method of illustrating complex Venn diagrams—each of the colored rows indicates a separate “set”, a horizontal bar chart indicates set size, a ball-and-stick diagram represents the different intersections, and a vertical bar chart indicates intersect size. In this case, note how both 20 DTR 9 °C and 28 DTR 9 °C sets have the highest number of uniquely differentially expressed genes (849 and 720 genes, respectively), followed by the 449 genes shared between all three temperatures. **C** UpsetR plot showing the distribution of genes in midguts. Note the difference with carcasses—the largest set size comes from genes uniquely expressed at 20 DTR 9 °C (1223 genes), followed by genes that are shared between all three temperatures (902 genes), followed by genes shared between 20 DTR 9 °C and 28 DTR 9 °C (485 genes).



expression of genes involved in metabolic and catabolic processes of small molecules (primarily organic acids including amino acids, oxoacids, carboxylic acids, and other organic acids). In addition, genes involved in energy generation via respiration (localized primarily in the mitochondria and surrounding membranes) and oxidoreductase functions (e.g., glutathione peroxidase, Supplementary Fig. 1, Supplementary

Data 1) were implicated. One exception to the patterns of expression exhibited in Trend 1 at the low temperature treatment was the smaller cluster 3, which showed unusual enrichment at day 9 post-blood meal. GO enrichment for this profile suggested gene products with functions in regulating the activity of peptidases involved in inhibiting the activity of serine proteases and metalloproteinases (Supplementary Fig. 1 and

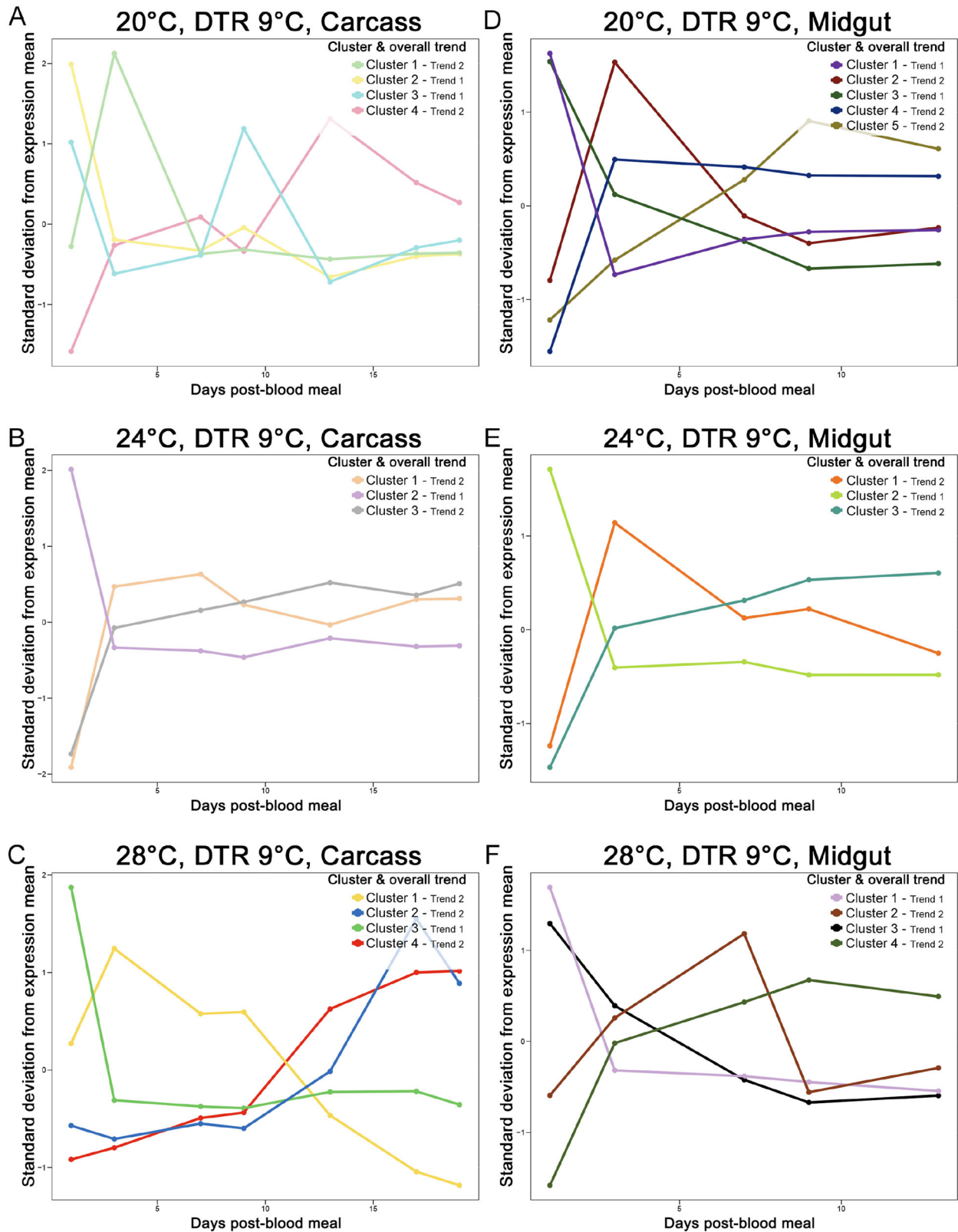


Fig. 3 | Expression profiles for statistically significant genes, separated by organ and temperature. Each graph represents a different temperature and tissue (as labeled), and each line on the graph represents a unique gene expression profile, as determined by Mfuzz and *K*-means clustering. The colored lines in each panel show temporal gene expression profiles for each cluster in the carcasses and midguts at 20 (A, D), 24 (B, E) and 28 (C, F) DTR 9 °C, respectively; x-axes show the sampled time-point in days post-blood meal, y-axis shows the standard deviation from the mean expression for that specific gene across the time-series (refer to Tables 1 and 2 for a

list of the number of genes within a specific cluster). Note the presence of two distinct trends (see the key on the top-right for each graph): Trend one is marked by high expression of genes one-day post-blood meal, followed by subsequent down-regulation and continued suppression throughout the remaining time-points. Trend two is marked by initial low expression of genes 1 day post-blood meal, followed by enrichment of genes at subsequent time-points, though the speed and degree of this enrichment are not necessarily consistent.

Table 1 | Overview of uniquely expressed gene clusters at each temperature and site of sampling

Tissue	Temperature	Total DEGs ($p < 0.05$)	Cluster number	Number of genes	Inferred trend	Number of genes profiled by GO analysis
Carcasses	20 DTR 9 °C	849	1	280	2	NA
			2	237	1	102
			3	105	1	13
			4	227	2	139
	24 DTR 9 °C	282	1	64	2	NA
			2	107	1	28
			3	111	2	42
	28 DTR 9 °C	720	1	347	2	198
			2	79	2	3
			3	159	1	36
			4	135	2	NA
	Midguts	20 DTR 9 °C	1223	1	313	1
2				238	2	69
3				241	1	162
4				204	2	22
5				227	2	67
24 DTR 9 °C		172	1	42	2	NA
			2	82	1	30
			3	48	2	3
28 DTR 9 °C		464	1	178	1	NA
			2	60	2	9
			3	76	1	3
			4	150	2	66

“Carcasses”/“Midguts”: Carcasses comprise all mosquito tissues pooled after the midguts were isolated from mosquitoes. “Temperature”: diurnal temperature range (DTR) of 9 °C implies fluctuations totaling + 5 °C/−4 °C, with temperatures over the 24 h averaging to 20 °C, 24 °C, and 28 °C (daily means). Therefore, “20 DTR 9 °C”, “24 DTR 9 °C”, “28 DTR 9 °C” indicate, respectively, daily maximums of 25 °C, 29 °C, and 33 °C, and daily minimums of 16 °C, 20 °C and 24 °C, which, over a 24 h period average to the daily mean of 20 °C, 24 °C and 28 °C. “Total DEGs ($p < 0.05$)”: total number of differentially expressed genes (DEGs) over time (also depicted as solitary points in Fig. 2B, C for carcasses and midguts respectively. “Cluster number”: genes with correlated trends in expression over time-based on K-means clustering. “Number of genes”: total number of genes in each cluster. “Inferred trend”: identifies clusters with gene expression profiles that followed Trend 1 or Trend 2 (Figs. 3 and 4); genes following Trend 1 were enriched by the blood meal before returning to mean expression levels for the remaining time-points: while genes following trend 2 were depleted by the blood meal, they were generally enriched thereafter, albeit with some variability at the later time-points compared to Trend 1 genes. “Number of genes profiled by GO analysis”: number of genes successfully assigned functions with gene ontology (GO) analysis.

NA not available.

Note the robustness of the clustering criteria is evident in the values in “Total DEGs” being identical to the sum of the values in “Number of genes” overall 4 clusters and temperature (e.g., Carcasses at 20 DTR 9 °C, Total DEGs of 849 = 280 (genes in cluster 1) + 237 + 105 + 227).

Supplementary Data 1), which are known to be associated with blood meal digestion, immunity, as well as oogenesis^{43,44}. In one notable observation, several of the GO terms identified at 20 DTR 9 °C have shown enriched gene and protein levels 1 day after a blood meal in other studies at higher average constant temperatures of 27–28 °C (DTR = 0 °C)^{43,45–48} but see refs. 10,11. Compared to the two clusters at 20 DTR 9 °C (342 genes), only cluster 2 (107 genes) at 24 DTR 9 °C (Fig. 3B) and cluster 3 (159 genes) at 28 DTR 9 °C (Fig. 3C) continued to follow Trend 1. GO enrichment of cluster 2 at 24 DTR 9 °C suggested genes involved in processes generally associated with localization and transport across membranes for instance, such as monoatomic ions (Supplementary Fig. 1, Supplementary Data 1). Cluster 3 at 28 DTR 9 °C also included the iron transport protein transferrin (Supplementary Data 2) that was shown to be critical for oogenesis in *An. culicifacies*, with another study demonstrating increased expression in *Aedes aegypti* at 30 °C compared to 20 °C^{49,50}.

Functional profiling of genes in clusters expressed in (i), carcasses, (ii), shared across all three temperatures and (iii), following Trend 1. When looking at genes shared across all temperatures, several gene expression profiles appear consistently present (Fig. 4A and Table 1). For

example, genes in cluster 3 for all three temperatures showed consistent enrichment 1-day post-blood meal, followed by depletion for the remainder of the sampling period. This is despite an apparent delay in blood meal digestion at 20 DTR 9 °C. GO annotations suggested that this cluster generally comprised highly enriched genes with products involved in localization and transport (proteins), post-translational modifications (e.g., glycosylation, ufmylation), and processes associated with the endoplasmic reticulum network (Supplementary Fig. 2). Amongst the GO terms that were highly represented at all three temperatures were biological processes pertaining to “signal peptide processing” and “protein ufmylation”, localized to the “signal peptidase complex” and with “protein disulfide isomerase activity” (and the related GO term of “intramolecular oxidoreductase activity transposing S-S bonds”) (Supplementary Fig. 2A, B, D and Supplementary Data 1). Most of the gene products associated with these terms are conserved across phyla and involved in protein folding, degradation, and trafficking to and from the endoplasmic reticulum^{51,52}. One exception to this is protein disulfide isomerase (Supplementary Data 2), which expresses dual oxidoreductase-isomerase functions and serves as an antioxidant in an *Aedes albopictus* cell line infected with DENV⁵³, but has also been shown to be essential for blood-feeding, survival, and oogenesis in ticks⁵⁴.

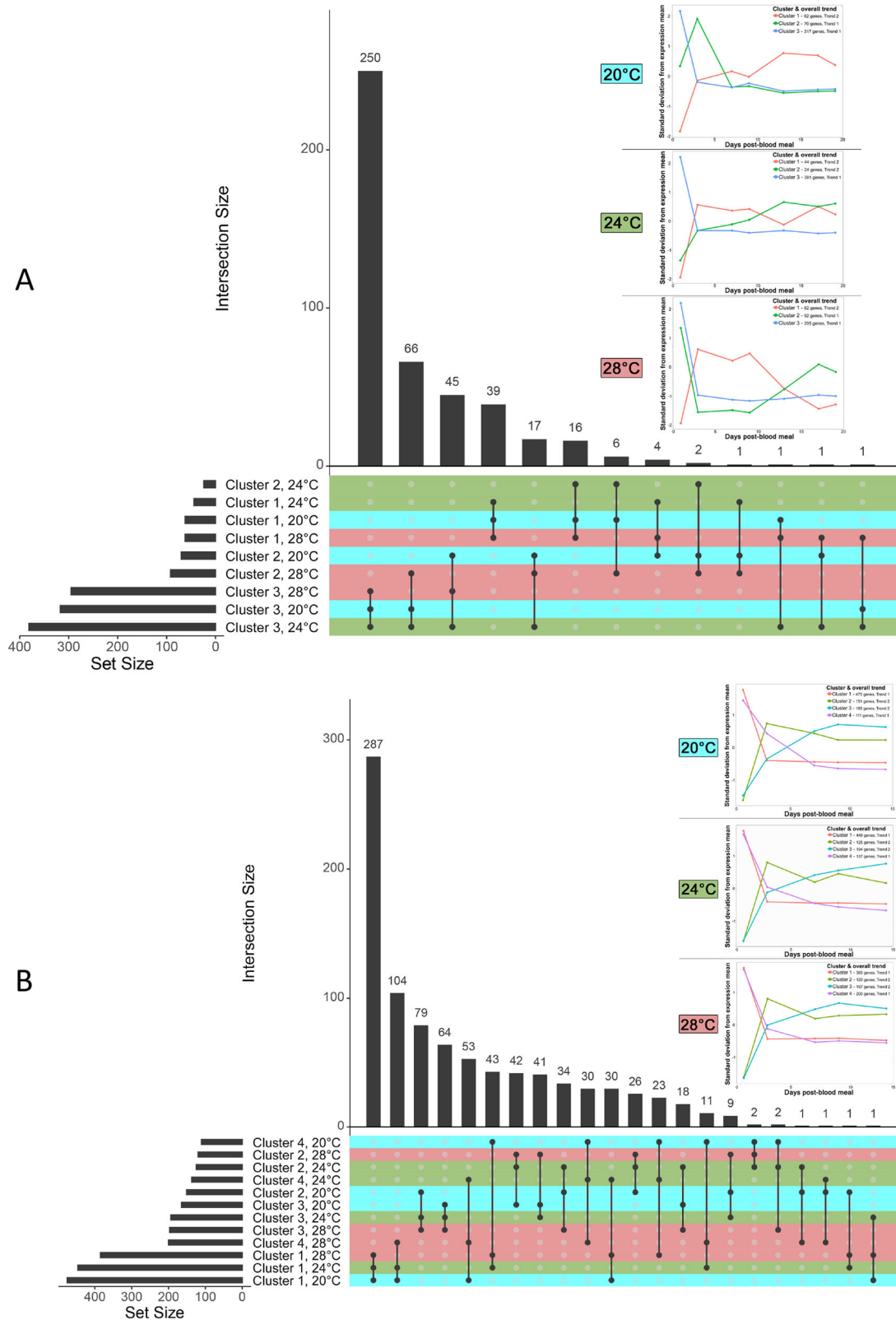


Fig. 4 | UpsetR plots and expression profiles for genes that showed differential expression at all three temperatures, separated by tissue. UpsetR sets are colored based on temperature, which corresponds to the color of the inset label. **A** Gene expression profiles from carcasses. Note how the largest intersection (250 genes) all correspond to genes from Cluster 3 at the different temperatures (right-most graphs of inset), which are genes that show immediate down-regulation after the first sampled time-point. Subsequent to this, the intersect sizes decrease significantly, with the second-largest set (66 genes) showing genes from Cluster 3 at 20 DTR 9°C and 24 DTR 9°C,

with these same genes appearing in Cluster 2 at 28 DTR 9°C, showing enrichment at later time-points. **B** Gene expression profiles from midguts. Note a more unified pattern of expression profiles, with each temperature having four profiles that show immediate depletion (Cluster 1) or enrichment (Cluster 2) genes, or a more gradual enrichment (Cluster 3) or depletion (Cluster 4) of genes. The largest intersect (287 genes) in this case comes from Cluster 1 at all three temperatures. The second-largest intersect (104 genes) show immediate depletion of expression at 20 DTR 9°C and 24 DTR 9°C, but a more gradual rate of depletion at 28 DTR 9°C.

Table 2 | Overview of gene clusters with shared gene expression profiles at each temperature and site of sampling

Tissue	Temperature	Total DEGs (p < 0.05)	Cluster number	Number of genes	Inferred trend	Number of genes profiled by Gene ontology analysis
Carcasses	20 DTR 9 °C	449	1	62	2	24
			2	70	2	25
			3	317	1	192
	24 DTR 9 °C	449	1	44	2	8
			2	24	2	6
			3	381	1	219
	28 DTR 9 °C	449	1	62	2	25
			2	92	1	20
			3	295	1	162
Midguts	20 DTR 9 °C	902	1	475	1	227
			2	151	2	19
			3	165	2	62
			4	111	1	52
	24 DTR 9 °C	902	1	448	1	228
			2	125	2	20
			3	194	2	143
			4	137	1	62
	28 DTR 9 °C	902	1	385	1	194
			2	120	2	2
			3	197	2	155
			4	200	1	95

"Carcasses"/"Midguts": Carcasses comprise all mosquito tissues pooled after the midguts were isolated from mosquitoes. "Temperature": diurnal temperature range (DTR) of 9 °C implies fluctuations totaling + 5 °C/−4 °C, with temperatures over the 24 h averaging to 20 °C, 24 °C, and 28 °C (daily means). Therefore, "20 DTR 9 °C", "24 DTR 9 °C", "28 DTR 9 °C" indicate, respectively, daily maximums of 25 °C, 29 °C, and 33 °C, and daily minimums of 16 °C, 20 °C, and 24 °C, which, over a 24 h period average to the daily mean of 20 °C, 24 °C and 28 °C. "Total DEGs (p < 0.05)": total number of differentially expressed genes (DEGs) over time (also depicted as solitary points in Fig. 2B, C for carcasses and midguts respectively. "Cluster number": genes with correlated trends in expression over time-based on K-means clustering. "Number of genes": total number of genes in each cluster. "Inferred trend": identifies clusters with gene expression profiles that followed Trend 1 or Trend 2 (Figs. 3 and 4): genes following Trend 1 were enriched by the blood meal before returning to mean expression levels for the remaining time-points: while genes following trend 2 were depleted by the blood meal, they were generally enriched thereafter, albeit with some variability at the later time-points compared to Trend 1 genes. "Number of genes profiled by GO analysis": number of genes successfully assigned functions with gene ontology (GO) analysis. Note that the analysis of shared gene clusters was restricted to genes that were expressed at all three temperatures (depicted in Fig. 2B, C by a single vertical line connecting all three nodes corresponding to the three temperatures). See legend to Table 1 for evaluating the robustness of K-means clustering criteria.

Functional profiling of Trend 2 genes in carcasses

Functional profiling of genes in clusters expressed in (i), carcasses, (ii), unique to each temperature and (iii), following Trend 2.

Genes in the remaining clusters can be grouped into members of Trend 2 (depleted day 1 post-blood meal, with expression increasing thereafter) and generally displayed more variability in the expression patterns as compared to Trend 1. Amongst the unique gene clusters in the carcasses, seven clusters appeared to follow this trend (Fig. 3A–C, see individual keys). For the clusters that GO profiling could be used (Supplementary Fig. 3), most of the gene products across all three temperatures were generally involved in aspects of nucleic acid (mainly DNA) metabolism, as well as processes localized to the nucleus and capable of binding nucleic acid such as transcription factors (Supplementary Data 1). For instance, following depletion at day 1 post-blood meal, expression increased over the 19 days for multiple transcription factors, including Nuclear transcription factor Y (20 DTR 9 °C, cluster 4), BZIP1 (24 DTR 9 °C, cluster 3), and Enhancer of yellow 2 (28 DTR 9 °C, cluster 4) (Supplementary Data 2). While little is known about the mechanisms of thermoregulation in animals, transcription factors in bacteria and plants play central roles in adjusting physiological responses to temperature changes⁵⁵. Nuclear transcription factor Y is critical for conferring desiccation tolerance in plants, with a recent study suggesting its involvement in regulating anhydrobiosis responses in an embryonic cell line from the larvae of the African midge, *Polypedilum vanderplanki*⁵⁶. Although the precise function of the BZIP1 transcription factor appears

to be unknown, in *Ae. aegypti*, its expression was enriched in the ovaries specifically after a blood meal⁵⁷. Taken together, this result suggests that genes in the clusters that followed Trend 2, were similar in their functional profiles and displayed temperature-dependent shifts in their dynamics of expression. For instance, at the coolest temperature (20 DTR 9 °C), expression of the 227 genes in cluster 4 increased until day 13 post-blood meal before declining again (Fig. 3A). At the intermediate temperature (24 DTR 9 °C), despite not as pronounced as the cooler temperature, the 111 genes in cluster 3 (Fig. 3B) increased in expression until 7 days post-blood meal before beginning to decline. Finally, at the warmest temperature (28 DTR 9 °C), the 347 genes in cluster 1, increased in expression until 3 days post-blood meal before beginning to decline to levels clearly lower than mean expression levels at that temperature by days 17 and 19 post-blood meal (Fig. 3C).

Functional profiling of genes in clusters expressed in (i), carcasses, (ii), shared across all three temperatures and (iii), following Trend 2.

Amongst the shared gene clusters in the carcasses, cluster 1 at all three temperatures and cluster 2 at 20 DTR 9 °C and 24 DTR 9 °C were depleted at day 1 post-blood meal, albeit with differences between the clusters at later time-points (Fig. 4A). Despite the small size of the clusters (24–70), in general, GO profiling suggests similar functional responses to the unique clusters, with gene products involved in nucleic acid metabolism in the nucleus and the binding of nucleic acids (histones, CDT1 DNA replication factor and DNA helicase) (Supplementary Fig. 4).

Functional profiling of Trend 1 genes in midguts

Functional profiling of genes in clusters expressed in (i), midguts, (ii), unique to each temperature and (iii), following Trend 1. Amongst the clusters of genes that were uniquely expressed in the midguts at each temperature, genes in clusters 1 and 3 at 20 DTR 9 °C and 28 DTR 9 °C and cluster 2 at 24 DTR 9 °C were characteristic of Trend 1 (Fig. 3D–F, see individual keys). Cluster 1 at 20 DTR 9 °C primarily comprised genes for transmembrane transporters that utilized ATP for the active transfer of solutes and ions (e.g., calcium-transporting ATPase, Supplementary Fig. 5A and Supplementary Data 1). However, genes in cluster 3 at the same temperature were involved in diverse biological processes such as cellular homeostasis (cell redox homeostasis), carbohydrate metabolism to energy generation (ATP), nucleoside and nucleotide metabolism (including purine synthesis), and other molecular functions to do with cellular respiration and oxidoreductase activity (Supplementary Fig. 5B). The GO term corresponding to cell redox homeostasis comprised genes coding for glutaredoxin, peroxiredoxin, superoxide dismutase, and protein disulfide isomerase (Supplementary Data 2), which are antioxidant proteins that protect against the oxidative environment created by blood meal digestion and *Plasmodium falciparum* infections^{58,59}. While GO profiling of genes in cluster 2 at 24 DTR 9 °C did not return any robust matches apart from genes with products that bound cyclic compounds such as nucleic acids (Supplementary Fig. 1C), it was unable to identify any GO terms corresponding to the 178 genes in cluster 1 at 28 DTR 9 °C. Analysis of the genes in cluster 3 at the 28 DTR 9 °C identified two genes for innexins (Supplementary Fig. 5D and Supplementary Data 2), a family of channel proteins (gap junction and non-junctional) exclusively expressed by invertebrates and essential for intercellular transfer of solutes and ions⁶⁰. Genes in the midguts associated with blood meal digestion also show delayed expression at the coolest temperature of 20 DTR 9 °C like Trend 1 genes expressed in carcasses.

Functional profiling of genes in clusters expressed in (i), midguts, (ii), shared across all three temperatures and (iii), following Trend 1. Amongst the four gene clusters that were shared across the three temperatures, clusters 1 and 4 followed Trend 1, but with gradual instead of immediate depletion of cluster 4 (Fig. 4B). For all three temperatures, cluster 1 comprised the largest number of genes with GO profiles reflecting blood meal digestion like catabolism (i.e., breakdown) of proteins, peptides, and functional groups associated with amino acids as part of the proteasome, as well as peptidase complexes for a wide variety of peptidolytic enzymes (Supplementary Fig. 6A, C, D and Supplementary Data 1). Genes shared across temperatures within cluster 4 were an extension of the previous cluster and included genes with oxidoreductase activities (Supplementary Fig. 6B, E, F). Cluster 4 at 28 DTR 9 °C was larger than the other Cluster 4 (200 genes) (Supplementary Fig. 1F), with GO analysis predicting the additional gene products to have peptidase functions and iron binding activities likely due to the breakdown of hemoglobin during blood meal digestion. This is in addition to ferritin and heme oxygenase activity (Supplementary Data 2), which was previously shown to be required for oogenesis in *An. gambiae*⁶¹.

Functional profiling of Trend 2 genes in midguts

Functional profiling of genes in clusters expressed in (i), midguts, (ii), unique to each temperature and (iii), following Trend 2. In the midguts, in addition to the 3 clusters at 20 DTR 9 °C, 2 clusters each at 24 and 28 DTR 9 °C can be considered members of Trend 2, with initial depletion followed by varying cluster-dependent trends in expression at later time-points. For example, depletion of the 238 genes in cluster 2 at 20 DTR 9 °C one-day after the blood meal was followed by significant enrichment at 3 days post-blood meal, albeit with reduced expression levels at the remaining time-points (Fig. 3D). Subsequent GO profiling suggested genes in this cluster were primarily associated with RNA synthesis and transcription in the nucleus (Supplementary Fig. 7A)

(Supplementary Data 1). In contrast, while the expression of genes in cluster 4 (204 genes) and cluster 5 (227 genes) at 20 DTR 9 °C showed a sharp increase at day 3 post-blood meal (Fig. 3), only genes in cluster 4 were expressed at below-average levels for the remaining time-points. While GO profiling was unable to identify clear functional associations for cluster 4, it suggested gene products in cluster 5 were associated with loading tRNA for protein translation as well as processing non-coding RNA (ncRNA) (Supplementary Fig. 7C). The importance of ncRNA in regulating gene expression and facilitating rapid responses to environmental change in mosquitoes is increasingly being recognized⁶². At 24 DTR 9 °C, clusters 1 and 3 were also members of Trend 2 (Fig. 3B). While GO profiling was unable to determine functional associations between the genes in cluster 1, only 3 genes in cluster 3 could be identified with roles in detection and response to external stimuli, potentially for finding nutrition, vertebrate hosts, and oviposition sites⁶³. At 28 DTR 9 °C, clusters 2 and 4 were identified as members of Trend 2. GO profiling of genes in cluster 2 identified roles in regulating peptidase activity, while genes in cluster 4 were associated with initialization and regulation of protein translation (e.g., Eukaryotic translation initiation factor 3), and localization to the ribosomes (e.g., 40S ribosomal proteins S7 and SA) (Supplementary Data 2). The identification of transcripts for 40S ribosomal protein S7 increasing in expression over time, specifically at 28 DTR 9 °C, indicates that caution should be used against relying on this gene as a reference/housekeeping gene^{57,64–66}.

Functional profiling of genes in clusters expressed in (i), midguts, (ii), shared across all three temperatures and (iii), following Trend 2.

Amongst clusters shared across all three temperatures, genes in clusters 2 and 3 were identified as members of Trend 2 (Fig. 4B). Genes in cluster 2 were primarily associated with protein translation and folding and showed rapid increases by day 3 post-blood meal before returning to levels close to the average for the duration of the study. While the products of genes in cluster 3 were also associated with translation and protein folding, their expression gradually increased over 13 days (Supplementary Fig. 8 and Supplementary Data 1).

Discussion

Overall gene expression profiles of the 97 samples suggested that 61% of the overall variability was dependent on the site of sampling (carcasses and midguts, 36% variance) and the effect of the blood meal (25%) (Fig. 1A). We observed effects of temperature and time post-blood meal on the transcriptional profiles of *Anopheles stephensi*. Analysis of expression patterns over time at 20 DTR 9 °C, 24 DTR 9 °C and 28 DTR 9 °C identified 1798, 1341 and 1671 genes in the carcasses, and 2810, 1418 and 1995 genes in the midguts differentially expressed, respectively. Of these genes that were differentially expressed, we noticed that many of these genes were shared across all 3 temperatures, between 2 of the 3 temperatures, or were unique to each temperature, in both the carcasses (Fig. 1B) and the midguts (Fig. 1C). We also noticed that a relatively fewer number of uniquely expressed genes at 24 DTR 9 °C in the carcasses (282 vs. 849 and 720 genes at 20 and 28 DTR 9 °C) and midguts (172 vs. 1223 and 464 genes at 20 and 28 DTR 9 °C) relative to the cooler and warmer temperature treatment suggests responding to the sub-optimal temperatures (20 and 28 DTR 9 °C) may be dependent on the expression of a larger and more diverse repertoire of gene products. There is some evidence for this from other systems. For example, the transcriptomics of larvae of the major African vector *An. gambiae* showed that, compared to the 2L+^a variants, the higher resistance to thermal stress in populations with the chromosomal inversion 2La was associated with expressing a larger repertoire of differentially expressed genes⁶⁷. Future research determining the extent to which this larger repertoire exerts a downstream effect on mosquito physiology or places greater demands for resources may prove to be useful. For instance, this shift may include pathways and mechanisms underlying differences in investment across life history processes to optimally respond and maintain fitness at sub-optimal temperatures.

We also found that the transcriptional profiles of genes that were shared among temperatures or were unique to a given temperature had two contrasting trends in the dynamics of expression over time in both midguts and carcasses (Fig. 2). Trend 1 comprised genes that were enriched at day 1 post-blood meal and repressed thereafter. Trend 2 comprised gene clusters that were repressed initially by the blood meal, with expression generally increasing thereafter, however, with greater variability among temperatures and time compared to the genes classified as Trend 1. GO annotations of the shared gene clusters in both carcasses and midguts at day 1 post-blood meal in Trend 1 suggest an association with blood meal digestion, processing and reducing the toxicity associated with the blood meal^{10,11,43,45–48,51–54}. In the carcasses for instance, clusters with shared expression patterns at all three temperatures comprise genes involved in protein localization, transport and post-translational modifications associated with the endoplasmic reticulum network (Supplementary Fig. 2), while the midguts are represented by genes with roles in blood meal digestion like catabolism (i.e., breakdown) of proteins, peptides, and functional groups associated with the proteasome, peptidase complexes for a wide variety of peptidolytic enzymes (Supplementary Fig. 6A, C, D and Supplementary Data 1), and genes with oxidoreductase activities (Supplementary Fig. 6B, E, F). By contrast, and maybe due to the larger size of the gene clusters, GO annotations of gene clusters that were unique to a given temperature returned more comprehensive overviews of gene expression for mosquitoes housed at 20 DTR 9 °C than the two warmer temperatures for the carcasses (Supplementary Fig. 1) as well as midguts (Supplementary Fig. 5). Further, these unique clusters exhibited enrichment of genes involved in metabolic and catabolic processes of small molecules (amino acids, oxoacids, carboxylic acids), energy generation via respiration and oxidoreductase functions^{11,43,46–48}. Taken together, these results suggest that cooler temperatures delay/prolong expression patterns of genes involved in blood meal processing, which could explain the reduced rate of blood meal digestion at 20 DTR 9 °C and the longer gonotrophic cycles observed in these mosquitoes at cooler temperatures more generally¹⁴. Additionally, comparison of GO terms enriched 1 day post-blood meal from other studies performed at higher average, but constant temperatures (27–28, DTR = 0 °C)^{10,11,43,45–48} revealed overlap with the GO terms identified here at 20 DTR 9 °C, but not at 24 DTR 9 °C and 28 DTR 9 °C: these results suggest rates of key biological processes derived at average temperatures (i.e., DTR = 0 °C) may be difficult to reconcile with rates derived from diurnal fluctuations (i.e., DTR > 0 °C)^{25–28}.

Genes exhibiting temporal dynamics of transcriptional profiles in Trend 2 that were repressed by the blood meal and then enriched thereafter, exhibited more variation in expression profiles over time compared to Trend 1 genes. In the carcasses, both shared and unique gene clusters were associated with biosynthetic pathways associated with GO terms related to nucleic acid (mainly DNA) metabolism, suggesting similar pathways and processes expressed at the three temperatures, but with different trends in expression over time. Protein synthesis and trafficking were also represented by shared gene clusters at all three temperatures in the midguts (Supplementary Fig. 8). While these processes are associated with mosquito's most critical life history trait, its gonotrophic cycle (e.g., see clusters 3 and 1 at 24 and 28 DTR 9 °C, respectively, Fig. 3 and Supplementary Fig. 3)^{68,69}, they are also enriched with ageing and oxidative stress in the Dipteran fruit fly, *Drosophila melanogaster* (cluster 4 at 20 DTR 9 °C, Fig. 3 and Supplementary Fig. 3)⁷⁰. Our results suggest Trend 2 genes in the carcasses may represent the temperature-specific rates of oogenesis, with the greater variability in expression levels at the later time-points potentially representing temperature-dependent differences in physiological aging⁷¹. Gene clusters in Trend 2 differentially expressed in mosquito midguts that were unique to a given temperature were characterized by biosynthetic pathways associated with RNA metabolism at 20 DTR 9 °C (Supplementary Fig. 7), and protein synthesis and trafficking at the warmest temperature of 28 DTR 9 °C (Supplementary Fig. 7). While these biosynthetic pathways are also elicited by a blood meal in the midguts of *Aedes aegypti*¹⁵, in general, a more comprehensive functional assessment of these gene clusters was limited by the inability to assign GO profiles. While this could be due to several

reasons⁷², of the 5 clusters we were unable to assign a GO profile to, all belonged to the uniquely expressed genes at the respective temperatures (Table 1).

There are some limitations to this work that need to be considered. First, the carcasses in our study were comprised of all mosquito tissues except the midgut, so we lack precision in outlining how transcriptional profiles are differentially expressed in other tissues throughout the mosquito body. We observed a greater number and diversity of genes differentially expressed in the midguts relative to the carcasses, which could be due to the presence of other tissues in the carcasses, resulting in a lower signal-to-noise ratio^{43,48}. We also observed a greater number and diversity of genes differentially expressed in the midguts relative to the carcasses, with a larger number of statistically significant genes being observed in midgut tissues. This could also be due to the sequencing depth chosen for our study with only highly expressed genes being retained and the remaining filtered out during sequencing or during the computational analysis post-sequencing. Nonetheless, the clear differences in gene expression profiles between the midguts and carcasses both before and after the blood meal indicate clear functional distinctions between systemic (carcass) and local (midgut) tissues that warrant more careful consideration before designing a study^{48,73}, and when using transcriptomic data to infer an organism's life history⁷³. A second limitation of our study is the use of pooled midgut and carcass samples rather than individual mosquitoes, which may have compromised the ability of our approach to detect genes expressed at low levels; however, in addition to being more cost-effective than sequencing individual mosquitoes, pooling may offer a larger and more robust overview of the biological variation within a group/treatment that can be assessed over independent biological replicates^{23,74}. Additionally, recognizing the dearth of studies that have examined gene expression over such a long duration and at various temperatures, our results nonetheless confirm (and build upon) findings from other, independent studies.

Conclusions

Our results have several important implications. First, our results have clear implications for the design of experiments testing the effects of temperature on mosquito life history and the transmission process. We identified differentially expressed genes that were shared across all three temperatures, suggesting that the expression of these genes was critical to regulating various processes of mosquito life history and that incorporating realistic diurnal temperature fluctuations influences gene expression profiles in distinct ways than constant temperature variation^{28,41,75}. Our study also cautions against the use of 40S ribosomal protein S7 as a reference / housekeeping gene for relative quantification of gene expression, as its temperature-dependent expression violates the assumption that its expression is insensitive to experimental perturbations. Second, our results suggest that mosquitoes may tolerate sub-optimal temperatures (cool and warm) by expressing a larger and more diverse repertoire of gene products. Thus, if mosquitoes expressing a smaller repertoire of gene products experience reduced physiological costs, this could help explain why the thermal optimum for survival and reproduction typically occurs at intermediate temperatures. Whether this is a general phenomenon outside of *An. stephensi* and other mosquito species occupying distinct ecological niches exhibit similar phenotypes remains an open question. Third, we noticed that clusters of genes that regulate blood-feeding, digestion, management of oxidative stress, etc. followed two general temporal trends that were temperature sensitive, reinforcing the many studies done to date that demonstrate the effects of temperature variation on various aspects of the mosquito life cycle. These temperature-induced shifts in gene expression dynamics could also have important implications for mosquito-malaria interactions, as malaria parasites rely on resources trafficked from the ovaries to the eggs and are constrained by mosquito immunity^{76,77}. Fourth, our study has implications for the design of genetically modified mosquitoes that rely on the expression of a given gene(s) to suppress field populations of mosquito vectors or replace them with mosquito populations that are resistant to human pathogens. Our work would suggest that these techniques could be

sensitive to thermal variation in the field and experience varying efficacy if deployed during different times of seasons or different geographic areas.

Data availability

Raw RNA sequencing datasets have been deposited in NCBI, under Bio-Project ID Number PRJNA1116119. All additional source data is included as supplementary data tables.

Received: 16 July 2024; Accepted: 7 January 2025;

Published online: 22 January 2025

References

- Sunday, J. M., Bates, A. E. & Dulvy, N. K. Thermal tolerance and the global redistribution of animals. *Nat. Clim. Change* **2**, 686–690 (2012).
- Kingsolver, J. G. & Buckley, L. B. Quantifying thermal extremes and biological variation to predict evolutionary responses to changing climate. *Philos. Trans. R. Soc. B-Biol. Sci.* **372** <https://doi.org/10.1098/rstb.2016.0147> (2017).
- Harvey, J. A. et al. Scientists' warning on climate change and insects. *Ecol. Monogr.* **93** <https://doi.org/10.1002/ecm.1553> (2023).
- González-Tokman, D. et al. Insect responses to heat: physiological mechanisms, evolution and ecological implications in a warming world. *Biol. Rev.* **95**, 802–821 (2020).
- Chen, J. L. & Lewis, O. T. Limits to species distributions on tropical mountains shift from high temperature to competition as elevation increases. *Ecol. Monogr.* **94** <https://doi.org/10.1002/ecm.1597> (2024).
- Deutsch, C. A. et al. Impacts of climate warming on terrestrial ectotherms across latitude. *Proc. Natl Acad. Sci. USA* **105**, 6668–6672 (2008).
- Brown, J. J., Pascual, M., Wimberly, M. C., Johnson, L. R. & Murdock, C. C. Humidity — The overlooked variable in the thermal biology of mosquito-borne disease. *Ecol. Lett.* **26**, 1029–1049 (2023).
- Mordecai, E. A. et al. Thermal biology of mosquito-borne disease. *Ecol. Lett.* **22**, 1690–1708 (2019).
- Logan, M. L. & Cox, C. L. Genetic constraints, transcriptome plasticity, and the evolutionary response to climate change. *Front. Genet.* **11**, 538226 (2020).
- Ferreira, P. G. et al. Temperature dramatically shapes mosquito gene expression with consequences for mosquito-Zika virus interactions. *Front. Microbiol.* **11**, 901 (2020).
- Wimalasiri-Yapa, B. et al. Temperature modulates immune gene expression in mosquitoes during arbovirus infection. *Open Biol.* **11**, 200246 (2021).
- WHO. World Malaria Report 2021 Report No. 978-92-4-004049-6, (World Health Organization, Geneva, Switzerland, 2021).
- Villena, O. C., Ryan, S. J., Murdock, C. C. & Johnson, L. R. Temperature impacts the environmental suitability for malaria transmission by *Anopheles gambiae* and *Anopheles stephensi*. *Ecology* e3685 <https://doi.org/10.1002/ecy.3685> (2022).
- Miazgowiec, K. L. et al. Age influences the thermal suitability of *Plasmodium falciparum* transmission in the Asian malaria vector *Anopheles stephensi*. *Proc. Biol. Sci.* **287**, 20201093 (2020).
- Pathak, A. K., Shiao, J. C., Thomas, M. B. & Murdock, C. C. Field relevant variation in ambient temperature modifies density-dependent establishment of *Plasmodium falciparum* gametocytes in mosquitoes. *Front. Microbiol.* **10**, 2651 (2019).
- Murdock, C. C., Blanford, S., Luckhart, S. & Thomas, M. B. Ambient temperature and dietary supplementation interact to shape mosquito vector competence for malaria. *J. Insect Physiol.* **67**, 37–44 (2014).
- Murdock, C. C., Sternberg, E. D. & Thomas, M. B. Malaria transmission potential could be reduced with current and future climate change. *Sci. Rep.* **6**, 27771 (2016).
- Shapiro, L. L. M., Whitehead, S. A. & Thomas, M. B. Quantifying the effects of temperature on mosquito and parasite traits that determine the transmission potential of human malaria. *PLoS Biol.* **15**, e2003489 (2017).
- Kirk, D., O'Connor, M. I. & Mordecai, E. A. Scaling effects of temperature on parasitism from individuals to populations. *J. Anim. Ecol.* **91**, 2087–2102 (2022).
- Johnson, L. R. et al. Understanding uncertainty in temperature effects on vector-borne disease: a Bayesian approach. *Ecology* **96**, 203–213 (2015).
- Sinka, M. E. et al. A new malaria vector in Africa: predicting the expansion range of *Anopheles stephensi* and identifying the urban populations at risk. *Proc. Natl Acad. Sci. USA* **117**, 24900–24908 (2020).
- Tadesse, F. G. et al. *Anopheles stephensi* mosquitoes as vectors of *Plasmodium vivax* and *falciparum*, Horn of Africa, 2019. *Emerg. Infect. Dis.* **27**, 603–607 (2021).
- Todd, E. V., Black, M. A. & Gemmell, N. J. The power and promise of RNA-seq in ecology and evolution. *Mol. Ecol.* **25**, 1224–1241 (2016).
- Oomen, R. A. & Hutchings, J. A. Genomic reaction norms inform predictions of plastic and adaptive responses to climate change. *J. Anim. Ecol.* **91**, 1073–1087 (2022).
- Salachan, P. V. & Sorensen, J. G. Molecular mechanisms underlying plasticity in a thermally varying environment. *Mol. Ecol.* **31**, 3174–3191 (2022).
- Sorensen, J. G., Schou, M. F., Kristensen, T. N. & Loeschcke, V. Thermal fluctuations affect the transcriptome through mechanisms independent of average temperature. *Sci. Rep.* **6**, 30975 (2016).
- Breitenbach, A. T., Bowden, R. M. & Paitz, R. T. Effects of constant and fluctuating temperatures on gene expression during gonadal development. *Integr. Comp. Biol.* **62**, 21–29 (2022).
- Shocket, M. S. et al. Mean daily temperatures can predict the thermal limits of malaria transmission better than rate summation. *bioRxiv* <https://doi.org/10.1101/2024.09.20.614098> (2024).
- Pathak, A. K., Shiao, J. C., Thomas, M. B. & Murdock, C. C. Cryogenically preserved RBCs support gametocytogenesis of *Plasmodium falciparum* in vitro and gametogenesis in mosquitoes. *Malar. J.* **17**, 457 (2018).
- Jiang, X. et al. Genome analysis of a major urban malaria vector mosquito, *Anopheles stephensi*. *Genome Biol.* **15**, 459 (2014).
- Andrews, S. *FastQC: A Quality Control Tool for High Throughput Sequence Data [Online]*. Available online at: <http://www.bioinformatics.babraham.ac.uk/projects/fastqc/> (2010).
- Kim, D., Paggi, J. M., Park, C., Bennett, C. & Salzberg, S. L. Graph-based genome alignment and genotyping with HISAT2 and HISAT-genotype. *Nat. Biotechnol.* **37**, 907–915 (2019).
- Liao, Y., Smyth, G. K. & Shi, W. featureCounts: an efficient general purpose program for assigning sequence reads to genomic features. *Bioinformatics* **30**, 923–930 (2014).
- Love, M. I., Huber, W. & Anders, S. Moderated estimation of fold change and dispersion for RNA-seq data with DESeq2. *Genome Biol.* **15**, 550 (2014).
- R Foundation for Statistical Computing. R: A Language and Environment for Statistical Computing (R Foundation for Statistical Computing, Vienna, Austria, 2021).
- Conway, J. R., Lex, A. & Gehlenborg, N. UpSetR: an R package for the visualization of intersecting sets and their properties. *Bioinformatics* **33**, 2938–2940 (2017).
- Kumar, L. & Futschik, M. E. Mfuzz: a software package for soft clustering of microarray data. *Bioinformatics* **2**, 5–7 (2007).
- Wickham, H. *ggplot2: Elegant Graphics for Data Analysis*. (Springer-Verlag, 2016).
- Reimand, J., Kull, M., Peterson, H., Hansen, J. & Vilo, J. g:Profiler—a web-based toolset for functional profiling of gene lists from large-scale experiments. *Nucleic Acids Res.* **35**, W193–W200 (2007).
- Blanford, J. I. et al. Implications of temperature variation for malaria parasite development across Africa. *Sci. Rep.* **3**, 1300 (2013).

41. Murdock, C. C., Paaijmans, K. P., Cox-Foster, D., Read, A. F. & Thomas, M. B. Rethinking vector immunology: the role of environmental temperature in shaping resistance. *Nat. Rev. Microbiol.* **10**, 869–876 (2012).
42. Paaijmans, K. P. et al. Influence of climate on malaria transmission depends on daily temperature variation. *Proc. Natl Acad. Sci. USA* **107**, 15135–15139 (2010).
43. Hixson, B. et al. A transcriptomic atlas of *Aedes aegypti* reveals detailed functional organization of major body parts and gut regional specializations in sugar-fed and blood-fed adult females. *eLife* **11**, e76132 (2022).
44. Santiago, P. B. et al. Proteases of haematophagous arthropod vectors are involved in blood-feeding, yolk formation and immunity—a review. *Parasit. Vectors* **10**, 79 (2017).
45. Majoline Tchioffo, T. et al. Differential transcriptomic response of *Anopheles arabiensis* to *Plasmodium vivax* and *Plasmodium falciparum* infection. *bioRxiv* <https://doi.org/10.1101/2021.05.28.446219> (2021).
46. Short, S. M., Mongodin, E. F., MacLeod, H. J., Talyuli, O. A. C. & Dimopoulos, G. Amino acid metabolic signaling influences *Aedes aegypti* midgut microbiome variability. *PLoS Negl. Trop. Dis.* **11**, e0005677 (2017).
47. Kumar, M. et al. Response to blood meal in the fat body of *Anopheles stephensi* using quantitative proteomics: toward new vector control strategies against malaria. *OMICS* **21**, 520–530 (2017).
48. Maccallum, R. M., Redmond, S. N. & Christophides, G. K. An expression map for *Anopheles gambiae*. *BMC Genomics* **12**, 620 (2011).
49. Rani, J. et al. Functional disruption of transferrin expression alters reproductive physiology in *Anopheles culicifacies*. *PLoS ONE* **17**, e0264523 (2022).
50. Muturi, E. J., Blackshear, M. Jr. & Montgomery, A. Temperature and density-dependent effects of larval environment on *Aedes aegypti* competence for an alphavirus. *J. Vector Ecol.* **37**, 154–161 (2012).
51. Guan, J. et al. Analysis of the functions of the signal peptidase complex in the midgut of *Tribolium castaneum*. *Arch. Insect Biochem. Physiol.* **97**, e21441 (2018).
52. Gerakis, Y., Quintero, M., Li, H. & Hetz, C. The UFMylation system in proteostasis and beyond. *Trends Cell Biol.* **29**, 974–986 (2019).
53. Chen, T.-H. et al. Antioxidant defense is one of the mechanisms by which mosquito cells survive dengue 2 viral infection. *Virology* **410**, 410–417 (2011).
54. Liao, M. et al. Functional analysis of protein disulfide isomerases in blood feeding, viability and oocyte development in *Haemaphysalis longicornis* ticks. *Insect Biochem. Mol. Biol.* **38**, 285–295 (2008).
55. Sengupta, P. & Garrity, P. Sensing temperature. *Curr. Biol.* **23**, R304–R307 (2013).
56. Yamada, T. G. et al. Identification of a master transcription factor and a regulatory mechanism for desiccation tolerance in the anhydrobiotic cell line Pv11. *PLoS ONE* **15**, e0230218 (2020).
57. Kojin, B. B., Biedler, J. K., Tu, Z. & Adelman, Z. N. Characterization of a female germline and early zygote promoter from the transcription factor bZip1 in the dengue mosquito *Aedes aegypti*. *Parasites Vectors* **13**, 353 (2020).
58. Champion, C. J. & Xu, J. The impact of metagenomic interplay on the mosquito redox homeostasis. *Free Radic. Biol. Med.* **105**, 79–85 (2017).
59. Surachetpong, W., Pakpour, N., Cheung, K. W. & Luckhart, S. Reactive oxygen species-dependent cell signaling regulates the mosquito immune response to *Plasmodium falciparum*. *Antioxid. Redox Signal.* **14**, 943–955 (2010).
60. Güiza, J., Barría, I., Sáez, J. C. & Vega, J. L. Innexins: expression, regulation, and functions. *Front. Physiol.* **9**, 1–9 (2018).
61. Spencer, C. S. et al. Characterisation of *Anopheles gambiae* heme oxygenase and metalloporphyrin feeding suggests a potential role in reproduction. *Insect Biochem. Mol. Biol.* **98**, 25–33 (2018).
62. Farley, E. J., Eggleston, H. & Riehle, M. M. Filtering the junk: assigning function to the mosquito non-coding genome. *Insects* **12**, 1–17 (2021).
63. Peach, D. A. H. & Blake, A. J. Mosquito (Diptera: Culicidae) vision and associated electrophysiological techniques. *Cold Spring Harb. Protoc.* **2023**, 107671 (2023).
64. Roy, S. et al. Direct and indirect gene repression by the ecdysone cascade during mosquito reproductive cycle. *Proc. Natl Acad. Sci. USA* **119**, e2116787119 (2022).
65. Calkins, T. L. & Piermarini, P. M. A blood meal enhances innexin mRNA expression in the midgut, malpighian tubules, and ovaries of the yellow fever mosquito *Aedes aegypti*. *Insects* **8** <https://doi.org/10.3390/insects8040122> (2017).
66. Liu, Z. et al. Transcriptome analysis of *Aedes albopictus* midguts infected by dengue virus identifies a gene network module highly associated with temperature. *Parasit. Vectors* **15**, 173 (2022).
67. Cassone, B. J. et al. Divergent transcriptional response to thermal stress by *Anopheles gambiae* larvae carrying alternative arrangements of inversion 2La. *Mol. Ecol.* **20**, 2567–2580 (2011).
68. de Carvalho, S. S. et al. *Aedes aegypti* post-emergence transcriptome: unveiling the molecular basis for the hematophagic and gonotrophic capacitation. *PLoS Negl. Trop. Dis.* **15**, e0008915 (2021).
69. Luo, Y. et al. Combined analysis of the proteome and metabolome provides insight into microRNA-1174 function in *Aedes aegypti* mosquitoes. *Parasit. Vectors* **16**, 271 (2023).
70. Huang, K. et al. RiboTag translational profiling of *Drosophila* oenocytes under aging and induced oxidative stress. *BMC Genomics* **20**, 50 (2019).
71. Barr, J. S. et al. Temperature and age, individually and interactively, shape the size, weight, and body composition of adult female mosquitoes. *J. Insect Physiol.* **148**, 104525 (2023).
72. Gaudet, P. & Dessimoz, C. in *The Gene Ontology Handbook* (eds. Christophe Dessimoz & Nives Škunca) 189–205 (Springer New York, 2017).
73. Sudmant, P. H., Alexis, M. S. & Burge, C. B. Meta-analysis of RNA-seq expression data across species, tissues and studies. *Genome Biol.* **16**, 287 (2015).
74. Takele Assefa, A., Vandesompele, J. & Thas, O. On the utility of RNA sample pooling to optimize cost and statistical power in RNA sequencing experiments. *BMC Genomics* **21**, 312 (2020).
75. Murdock, C. C., Moller-Jacobs, L. L. & Thomas, M. B. Complex environmental drivers of immunity and resistance in malaria mosquitoes. *Proc. Biol. Sci.* **280**, 20132030 (2013).
76. Werling, K. et al. Development of circulating isolates of *Plasmodium falciparum* is accelerated in *Anopheles* vectors with reduced reproductive output. *PLoS Negl. Trop. Dis.* **18**, e0011890 (2024).
77. Kamiya, T., Paton, D. G., Catteruccia, F. & Reece, S. E. Targeting malaria parasites inside mosquitoes: ecoevolutionary consequences. *Trends Parasitol.* <https://doi.org/10.1016/j.pt.2022.09.004> (2022).

Acknowledgements

Funding for this work was provided by the University of Georgia and the NIH NIAID grants (5R01AI110793, 5R01AI153444). The funding bodies did not have any say in the design of the study and collection, analysis, interpretation of data or in writing the manuscript. A.K.P. was also supported by the Georgia Research Alliance, the SporoCore and 5P30AI168386-02 (sub-award A866298). G.L.H. was supported by the BBSRC (BB/V011278/1, BB/X018024/1, and BB/W018446/1), the UKRI (20197), a Royal Society Wolfson Fellowship (RSWF\R1\180013), the

NIHR (NIHR2000907), and the Bill and Melinda Gates Foundation (INV-048598).

Author contributions

Designed research: A.K.P., C.C.M. Performed research: A.K.P., R.S., J.C.S. Contributed new reagents or analytical tools: M.B.T., G.L.H. Analyzed data: S.Q., G.L.H. Wrote the paper: A.K.P., S.Q., C.C.M. Funding acquisition: C.C.M., M.B.T., G.L.H.

Competing interests

The authors declare no competing interests.

Additional information

Supplementary information The online version contains supplementary material available at <https://doi.org/10.1038/s42003-025-07477-2>.

Correspondence and requests for materials should be addressed to Ashutosh K. Pathak.

Peer review information *Communications Biology* thanks Luz García-Longoria and the other, anonymous, reviewer(s) for their contribution to the peer review of this work. Primary handling editors: Dr Hannes Schuler and Dr Ophelia Bu. A peer review file is available.

Reprints and permissions information is available at <http://www.nature.com/reprints>

Publisher's note Springer Nature remains neutral with regard to jurisdictional claims in published maps and institutional affiliations.

Open Access This article is licensed under a Creative Commons Attribution-NonCommercial-NoDerivatives 4.0 International License, which permits any non-commercial use, sharing, distribution and reproduction in any medium or format, as long as you give appropriate credit to the original author(s) and the source, provide a link to the Creative Commons licence, and indicate if you modified the licensed material. You do not have permission under this licence to share adapted material derived from this article or parts of it. The images or other third party material in this article are included in the article's Creative Commons licence, unless indicated otherwise in a credit line to the material. If material is not included in the article's Creative Commons licence and your intended use is not permitted by statutory regulation or exceeds the permitted use, you will need to obtain permission directly from the copyright holder. To view a copy of this licence, visit <http://creativecommons.org/licenses/by-nc-nd/4.0/>.

© The Author(s) 2025